Global Gyrofluid Simulations of Turbulence in Tokamak Plasmas

Sehoon Ko
Co-author: S.S. Kim, Hogun Jhang, J.-H. Kim, J. Seo, and H. Kaang
Korea Institute of Fusion Energy

2023 BOUT++ WORKSHOP, JAN 9-11

Contents

- A brief history of GLF simulations at KFE
- Introduction
- 3+1 Global Gyro-Landau Fluid model
- Neoclassical Equilibrium
- Ion Temperature Gradient- driven Linear/Nonlinear Simulations
- Flux-driven Nonlinear ITG Simulations
- Internal Transport Barrier Formation by An External Vorticity Source
- Summary

A brief history of GLF simulations at KFE

- Fluid simulations of turbulent transport initiated from 2010
  - ➢ Main tool: TRB code [X Garbet et al PoP 2001]
  - ➢ Study of ITB formation and intrinsic rotation **[SS Kim et al NF 2011; S Tokunaga et al PoP 2012; GY Park et al PoP 2015; H Jhang et al PoP 2019]**
    - → Problem of non-resonant modes: a motivation switching to BOUT++
- BOUT++ simulations have been applied various areas
  - ➢ NL physics of edge pedestal collapse and transport
    - ✓ **Elucidate the magnetic field stochastization mechanism and its impact on transport [T Rhee et al NF 2015; JW Kim et al PoP 2018]**
    - ✓ **RMP [JH Kim et al NF 2019]/ZF [H Jhang et al NF 2017] effects on pedestal collapse**
  - ➢ Electromagnetic effects on enhanced $k_{||}$ symmetry breaking [H Kaang et al PoP 2018]
  - ➢ Fundamental physics of plasma turbulence [T Tran et al PoP 2019; T Tran et al PPCF 2020]
  - ➢ Development of a working global flux-driven GF code → focus on this talk

Progress in recent theoretical development

- A conservative formulation of a system of GF equations and an in-depth analysis of the effect of parallel closures on GF energetics [SS Kim& H Jhang PoP 2020]
  - Fluid closure affects directly to field energy → a source of spurious field energy
  - A closure necessitates additional FLR closure to be consistent with the field energy conservation
  - Zonal flow closure consistent with 4+2 energetics under investigation

- Impact of magnetic field inhomogeneity on gyro-averaging operator [H Jhang & SS Kim PoP 2022]

  → Modification of GK Poisson and Ampere law under construction

- Heat source effects on RH residual zonal flow [SS Kim, S Ku, H Jhang, NF 2022]

⇨ Development and implementation of a closure including the heat source effect on-going

Introduction

- To study long-time qualitative physics with low computational cost, we have been developing a 3+1 Global Gyro-Landau Fluid code using BOUT++ framework.

- We match linear ITG mode growth rates with gyrokinetic and gyrofluid results adjusting hyper-viscosity and neoclassical poloidal flow and Pfirsch-Schulter return flow at an equilibrium are satisfied.

- We achieve a nonlinear steady state of gradient-driven ITG turbulence in the global simulation. A simulation without an external heating is carried and a final state of $R_0 / L_{Ti} \sim 5$ is obtained and similar to that of gyrokinetic code, gKPSP.

- In flux-driven simulations with various heating powers, heat transport shows characteristic of self-organized criticality (SOC)-like avalanche.

- We simulate internal transport barrier induced by an external vorticity source. After vorticity source injection, avalanche heat transport is reduced and stationary zonal flow pattern is formed in a global region

3+1 Global Gyro-Landau Fluid model

- Gyrocenter density equation

$$\frac{\partial \tilde{n}}{\partial t} + \boldsymbol{V_\Phi} \cdot \nabla n + n_0 B \partial_\parallel \frac{\tilde{V}_\parallel}{B} + n_0 K(\Phi) + K\left(\tilde{P}_{i\parallel} + \tilde{P}_{i\perp}\right) = -\mu_{h.v.} \nabla^4 \tilde{n}$$

- Gyrocenter parallel velocity equation

$$\frac{\partial \tilde{V}_\parallel}{\partial t} + \boldsymbol{V_\Phi} \cdot \nabla V_\parallel + \partial_\parallel \Phi + \frac{1}{n_0} \partial_\parallel \tilde{P}_{i\parallel} + \left(\tilde{T}_{i\perp} - \tilde{T}_{i\parallel}\right) \partial_\parallel \ln B + 4 T_0 K\left(\tilde{V}_\parallel\right) = -\mu_{h.v.} \nabla^4 \tilde{V}_\parallel + S_V(\tilde{V}_\parallel)$$

- Gyrocenter parallel temperature equation

$$\frac{\partial \tilde{T}_{i\parallel}}{\partial t} + \boldsymbol{V_\Phi} \cdot \nabla T_{i\parallel} + \frac{B}{n_0} \partial_\parallel \frac{\tilde{q}_{i\parallel}}{B} + 2 T_0 B \partial_\parallel \frac{\tilde{V}_\parallel}{B} + \frac{2}{n_0}\left(\tilde{q}_{i\perp} + P_0 \tilde{V}_\parallel - P_0 V_\parallel^{neo}\right) \partial_\parallel \ln B + 2 n_0 K(\Phi) + 3 \frac{T_0}{n_0} K\left(\tilde{P}_{i\parallel}\right) - \frac{T_0}{n_0} K\left(\tilde{P}_{i\perp}\right) + T_0 K\left(3 \tilde{T}_{i\parallel} + \tilde{T}_{i\perp}\right) = -\mu_{h.v.} \nabla^4 \tilde{T}_{i\parallel} + S_T(\tilde{T})$$

- Gyrocenter perpendicular temperature equation

$$\frac{\partial \tilde{T}_{i\perp}}{\partial t} + \boldsymbol{V_\Phi} \cdot \nabla T_{i\perp} + \frac{B}{n_0} \partial_\parallel \frac{\tilde{q}_{i\perp}}{B} - \frac{1}{n_0}\left(\tilde{q}_{i\perp} + P_0 \tilde{V}_\parallel\right) \partial_\parallel \ln B + n_0 K(\Phi) + 2 \frac{T_0}{n_0} K\left(\tilde{P}_{i\perp}\right) - \frac{T_0}{n_0} K\left(\tilde{P}_{i\parallel}\right) + T_0 K\left(\tilde{T}_{i\parallel} + 2 \tilde{T}_{i\perp}\right) = -\mu_{h.v.} \nabla^4 \tilde{T}_{i\perp} + S_T(\tilde{T})$$

where $f = f_0 + \tilde{f}$, $\Phi = \langle \phi \rangle = \frac{1}{1 - 0.5 \rho_i^2 \nabla_\perp^2} \phi$, $\boldsymbol{V_\Phi} = \frac{1}{B} \boldsymbol{b} \times \nabla \Phi$,

$K(f) = \frac{1}{2B}(\boldsymbol{b} \times \boldsymbol{\kappa} + \boldsymbol{b} \times \nabla \ln B) \cdot \nabla f$, $S_T(\tilde{T})$ ($S_V(\tilde{V}_\parallel)$): sum of heat (momentum) source, sink and core diffusion

Some features for the model

- Developed under BOUT++ framework [B. Dudson et al. CPC'09].
- Gyrokinetic Poisson equation for n=0 potential

$$-\nabla_\perp \cdot \frac{\rho_i^2}{\lambda_{Di}^2} \nabla_\perp \phi + \frac{1}{\lambda_{De}^2}\left(\phi - \langle\phi\rangle_f\right) = 4\pi e \langle\tilde{n}\rangle$$

- To construct gyrokinetic Poisson matrix in (r,θ) plane, 4th order finite difference method and Simpson's rule are adopted.
  - Direct matrix inversion (UMFPACK)

- Finite Larmor Radius (FLR) terms are partially considered in the model for numerical stability.
- Hyper-viscous damping terms are introduced for numerical stability and to reduce high k-modes
- Parallel Landau damping is taken into account.
- Residual zonal flow closure is not included but neoclassical poloidal damping and PS return flows are considered.

Neoclassical poloidal flow & Pfirsch-Schluter return flow at equilibrium

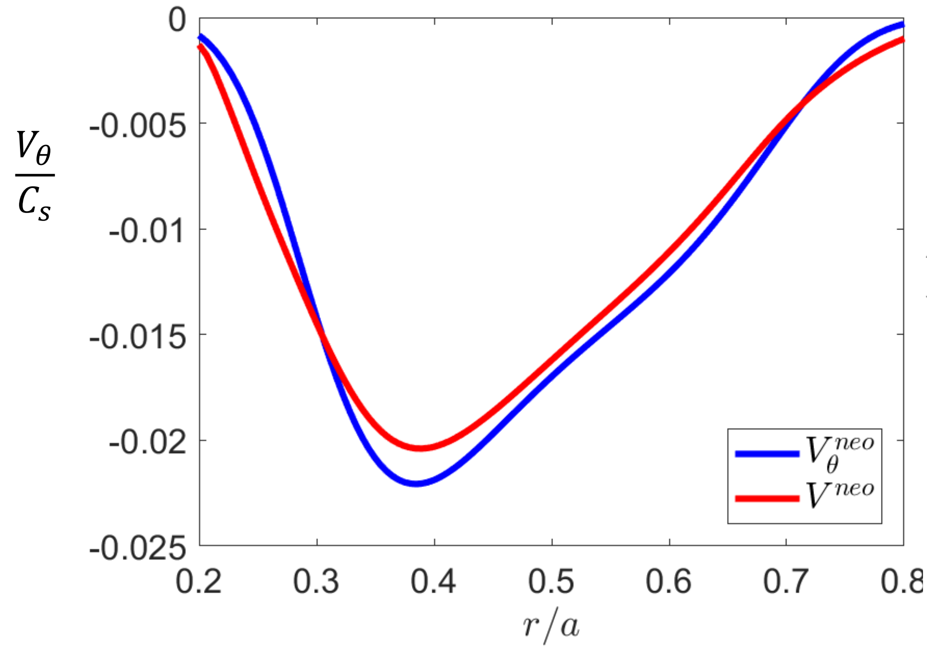

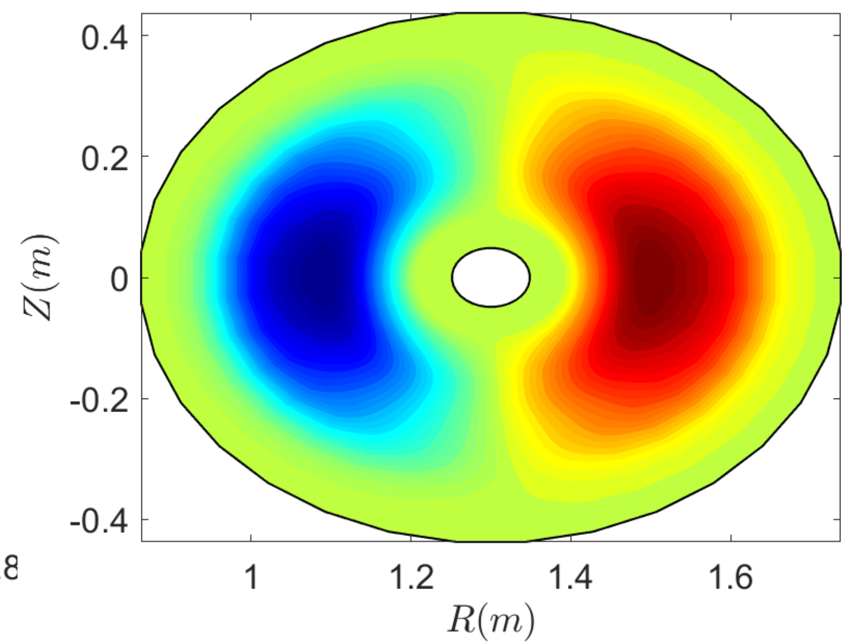

$$V_\theta^{neo} = 1.17 \frac{\hat{\theta} \cdot \vec{b} \times \nabla T_i}{eB} \qquad V_{PS} = RB_T \left(-\frac{d\Phi}{d\psi} - \frac{1}{n_i}\frac{dP_i}{d\psi} \right) \left(1 - \frac{B^2}{\langle B^2 \rangle_f} \right)$$

- We confirm that neoclassical equilibrium is achieved.
  - Poloidal flow is generated at neoclassical level.
  - Parallel flow (.i.e. P-S return flow) is developed to match $\nabla \cdot (n\vec{V}) = 0$.

Ion temperature gradient driven linear/nonlinear simulations

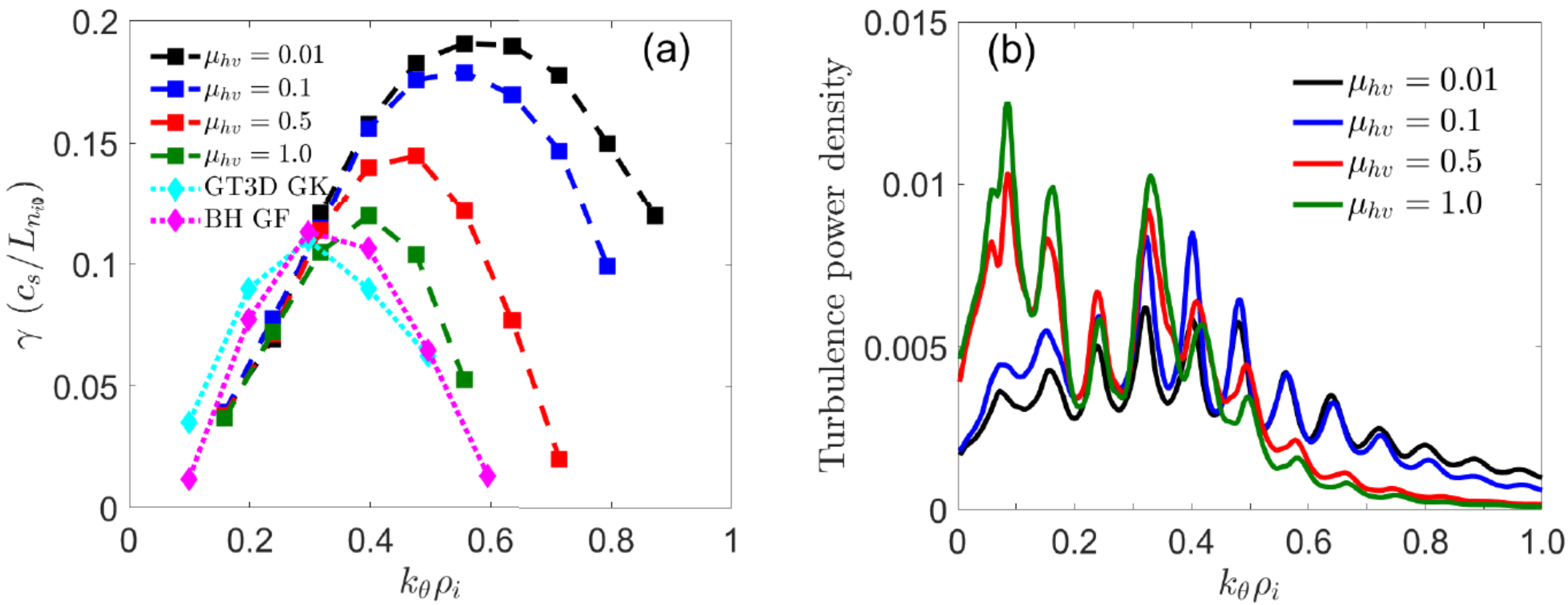

- Simulations are carried using cyclone base parameters ($q = 1.4, \hat{s} = \frac{r}{q}\frac{dq}{dr} = 0.772$, $R_0/L_{T_i} = 6.92$, $R_0/L_{n_e} = 2.22$).
  - ➢ As hyper-viscosity increases, linear ITG growth rate reduces to those of gyrokinetic simulation and gyrofluid simulation of Beer and Hammett and turbulence power density of high k-modes also decreases and k value of maximum turbulent power intensity moves to lower k value in nonlinear simulation.

Ion heat conductivity of gradient-driven nonlinear ITG turbulent simulations

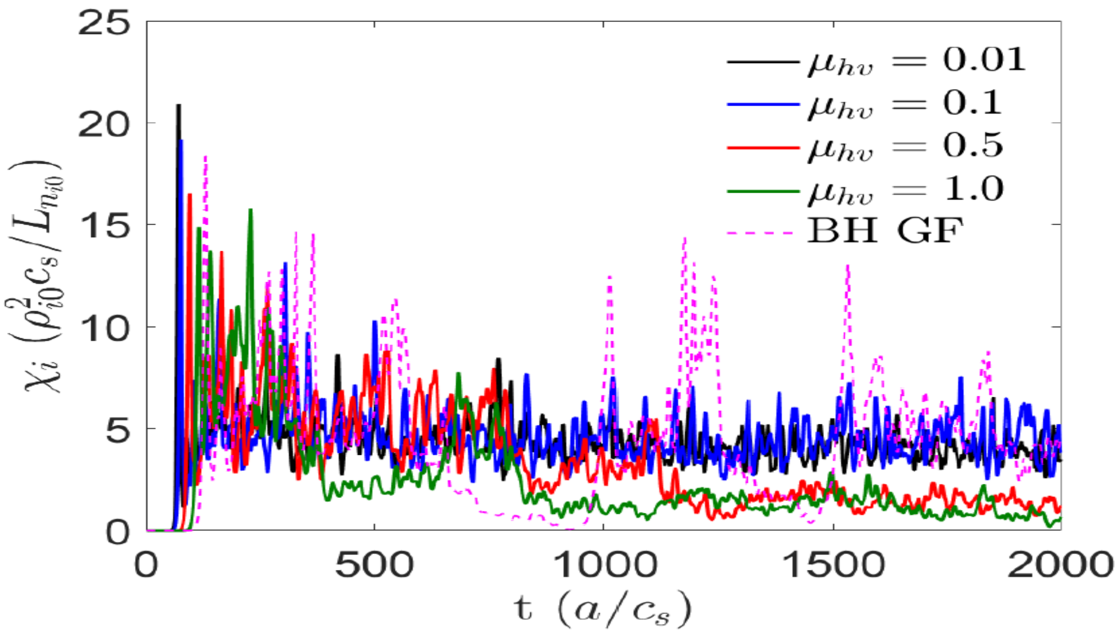

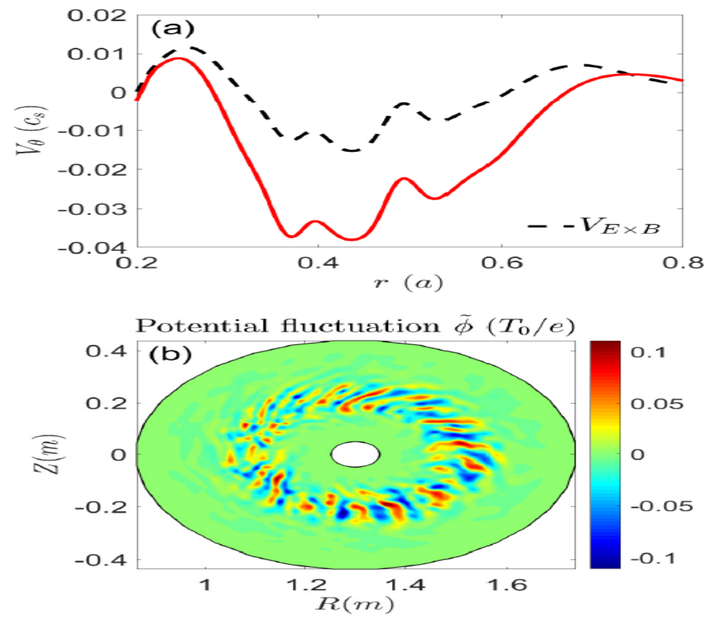

- As hyper-viscosity increases, potential fluctuations are reduced (mostly high k-modes) and ion heat conductivity decreases correspondingly.
  - For $\mu_{h.v.}$=1.0, ion heat conductivity is comparable to that of local gyrokinetic simulation.
  - $\mu_{h.v.}$=1.0 is chosen for hyper-viscosity hereafter.
- A simulation using ‘3+1’ gyrofluid model by Beer and Hammett shows that ion heat conductivity bursts irregularly and it may come from non-conservative model or/and numerical issues.
- For $\mu_{h.v.}$=1.0, poloidal ExB velocity shows a zonal flow pattern and a potential fluctuation is regulated by the zonal flow.

Linear/Non-linear ITG turbulence threshold with $\mu_{h.v.}$=1.0

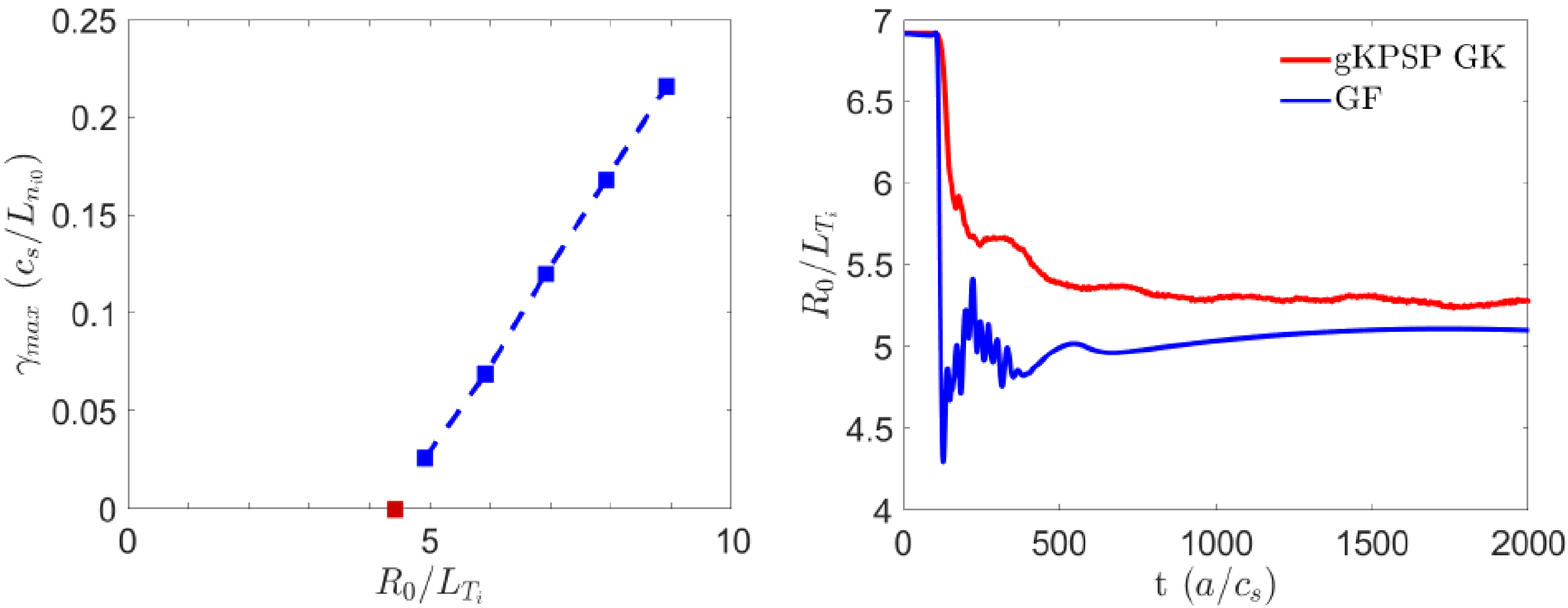

- Maximum growth rate of linear ITG turbulence, γ_{max} increases as R_0/L_{T_i} increases.
  - ➢ The threshold is $R_0/L_{T_{i,crit}}$ ~4.4, similar to $R_0/L_{T_{i,crit}}$ ~4 of gyrokinetic result.
- Nonlinear ITG turbulence simulation without an external heating source is carried for comparison of gyrokinetic simulation, gKPSP, nullifying n=0 potential.
  - ➢ Nonlinear critical gradient of the simulation, $R_0/L_{T_{i,crit}}$ ~5.03, similar to $R_0/L_{T_{i,crit}}$ ~5.25 of gKPSP result.

Flux-driven simulation setting

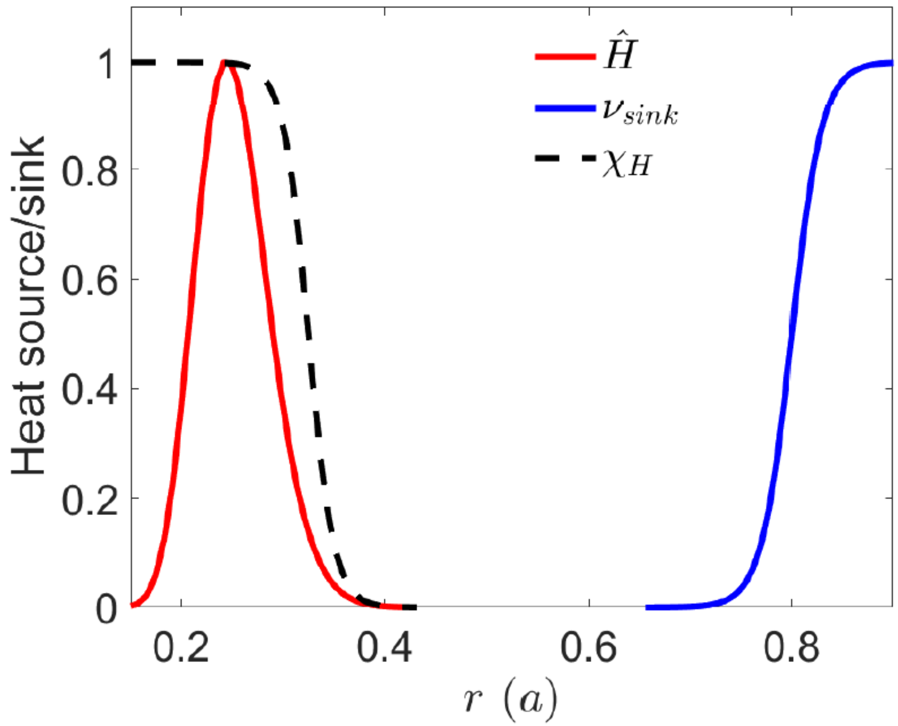

- $S(T) = H + \chi_H \frac{d^2\langle T\rangle}{dr^2} - \nu_{sink}\langle T\rangle$
  - $H = H_0\widehat{H}$, $\chi_H = 5m/s^2$, and $\nu_{sink} = 1$ in code unit (c_s/a).

- We obtain nonlinear steady state of flux-driven ITG simulations with various heating powers.

Flux driven simulation with 2MW heating power (1)

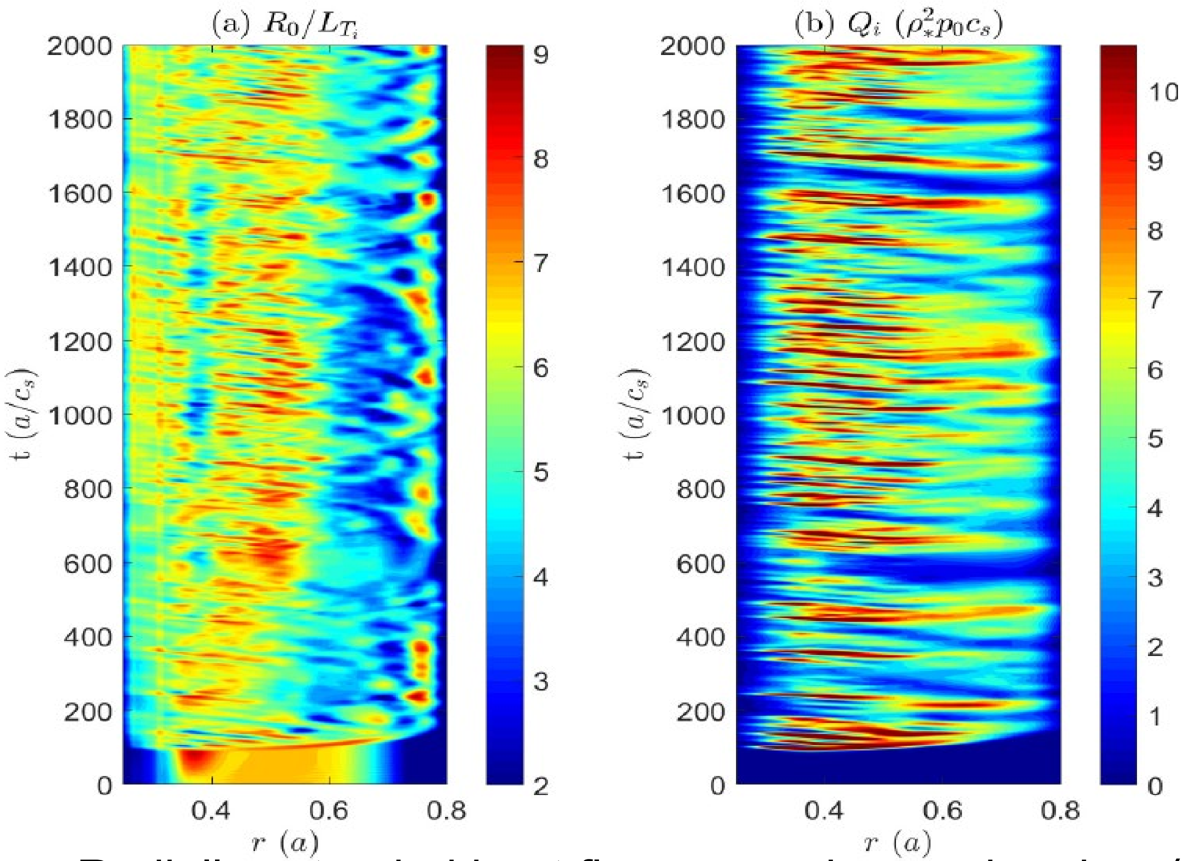

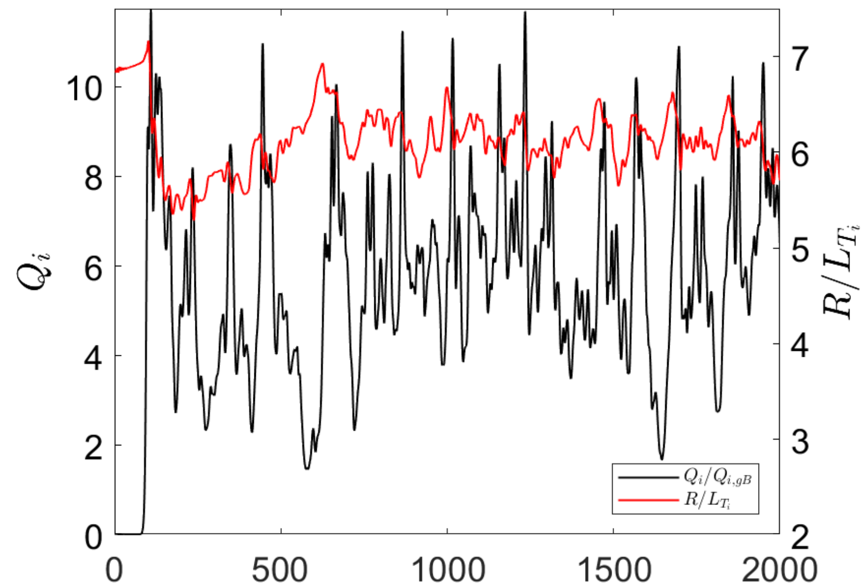

- Radially extended heat fluxes are observed and R_0/L_{T_i} varies correspondingly in spatio-temporal plots.
  - ➢ Prolonged corrugation of R_0/L_{T_i} is not clearly observed. ➔ Absence of residual ZF closure in GF model?
- Plot, spatially averaged from 0.4 r/a to 0.6 r/a, shows that R_0/L_{T_i} grows and collapse after each heat bursts out.

Flux driven simulation with 2MW heating power (2)
-Probability distribution function and power spectral density

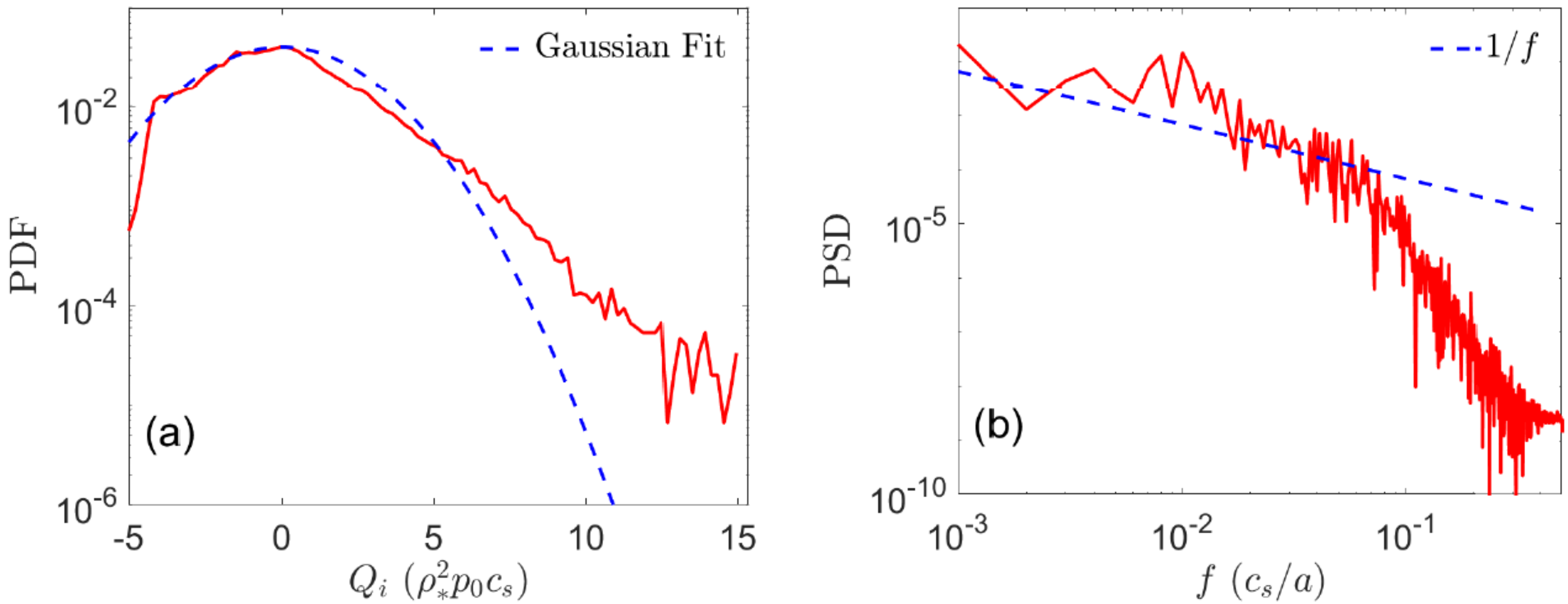

- Non-Gaussian PDF of heat flux with skewness, S=0.768, and kurtosis, K=4.325.
- Power spectral density shows 1/f dependency from low to intermediate frequency range.

➔ Self-organized criticality (SOC)-like heat avalanche

- PDF and PSD are evaluated using heat flux from 0.4 r/a to 0.6 r/a for 1000 steps after 1000 a/c_s.

Internal transport barrier formation by an external vorticity source (1)
-Additional equations

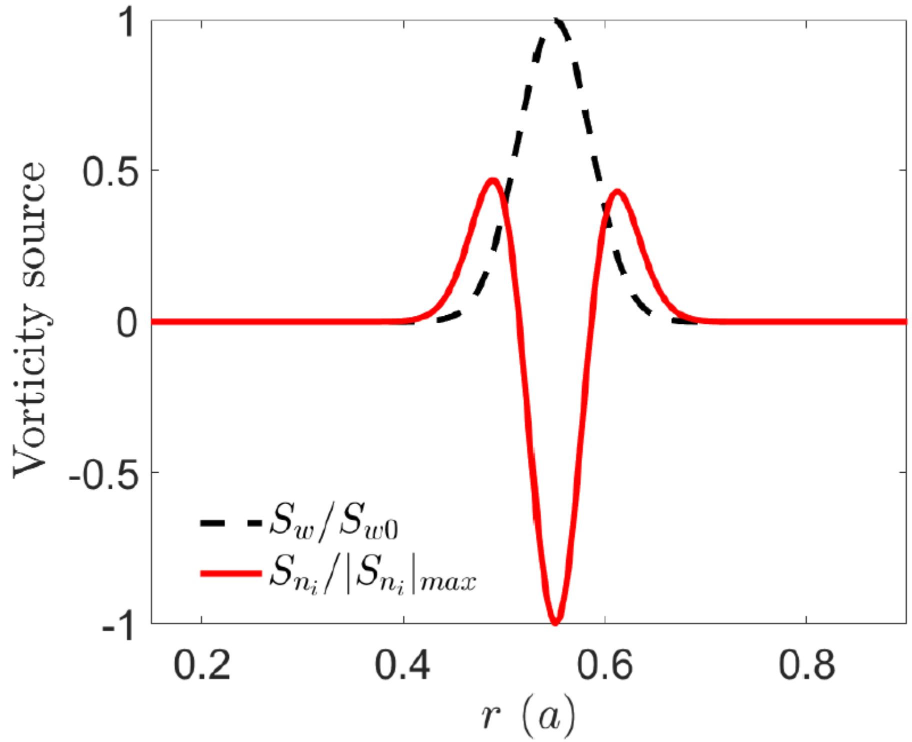

- $\frac{\partial W}{\partial t} = S_{n_i} = \rho_*^2 \nabla_\perp^2 S_w$ Vorticity equation
- $-\nabla_\perp \cdot \frac{\rho_i^2}{\lambda_{di}^2} \nabla_\perp \phi + \frac{1}{\lambda_{de}^2}(\phi - \langle\phi\rangle) = 4\pi e(\langle\tilde{n}\rangle + W)$ gyrokinetic Poisson equation

➔ solved simultaneously with the gyrofluid equations.

Internal transport barrier formation by an external vorticity source (2)

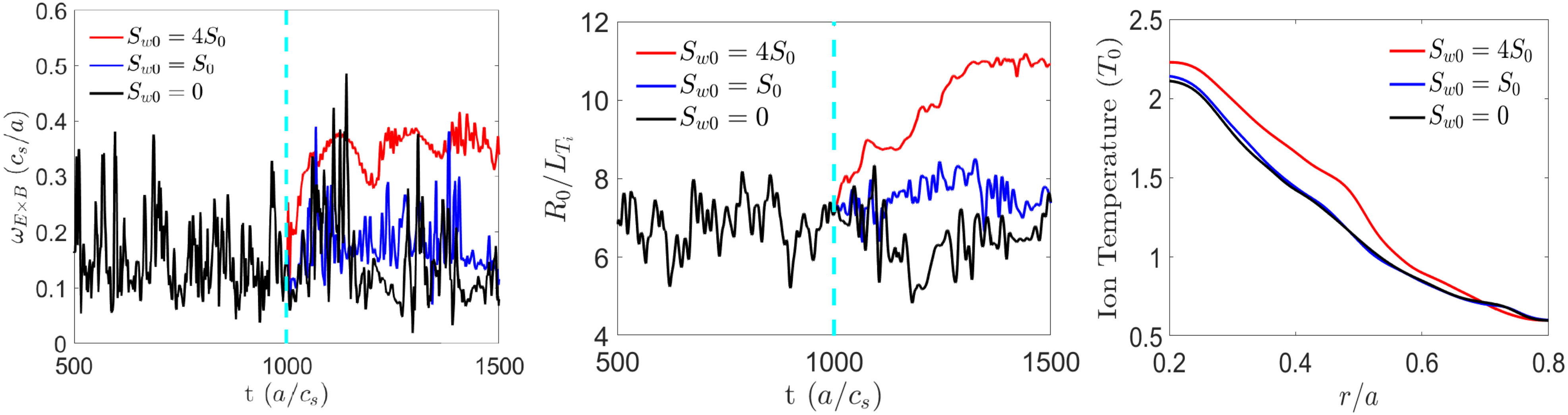

- After flux-driven ITG steady state with 4MW is achieved, three different vorticity sources ($4S_0$,S_0,0) are injected, where $S_0=0.1n_0c_s/a$.
- For strong vorticity injection ($S_{w0} = 4S_0$), ExB flow shear develops strongly, R_0/L_{T_i} increases as time goes by and finally internal transport barrier of ion temperature is formed at 1500 a/c_s.

  ➔ ITB builds up from 0.49 r/a to 0.56 r/a in a monotonic q profile by strong vorticity injection.
- ExB flow shear and R_0/L_{T_i} are averaged in the ITB region.

Internal transport barrier formation by an external vorticity source – Strong vorticity source

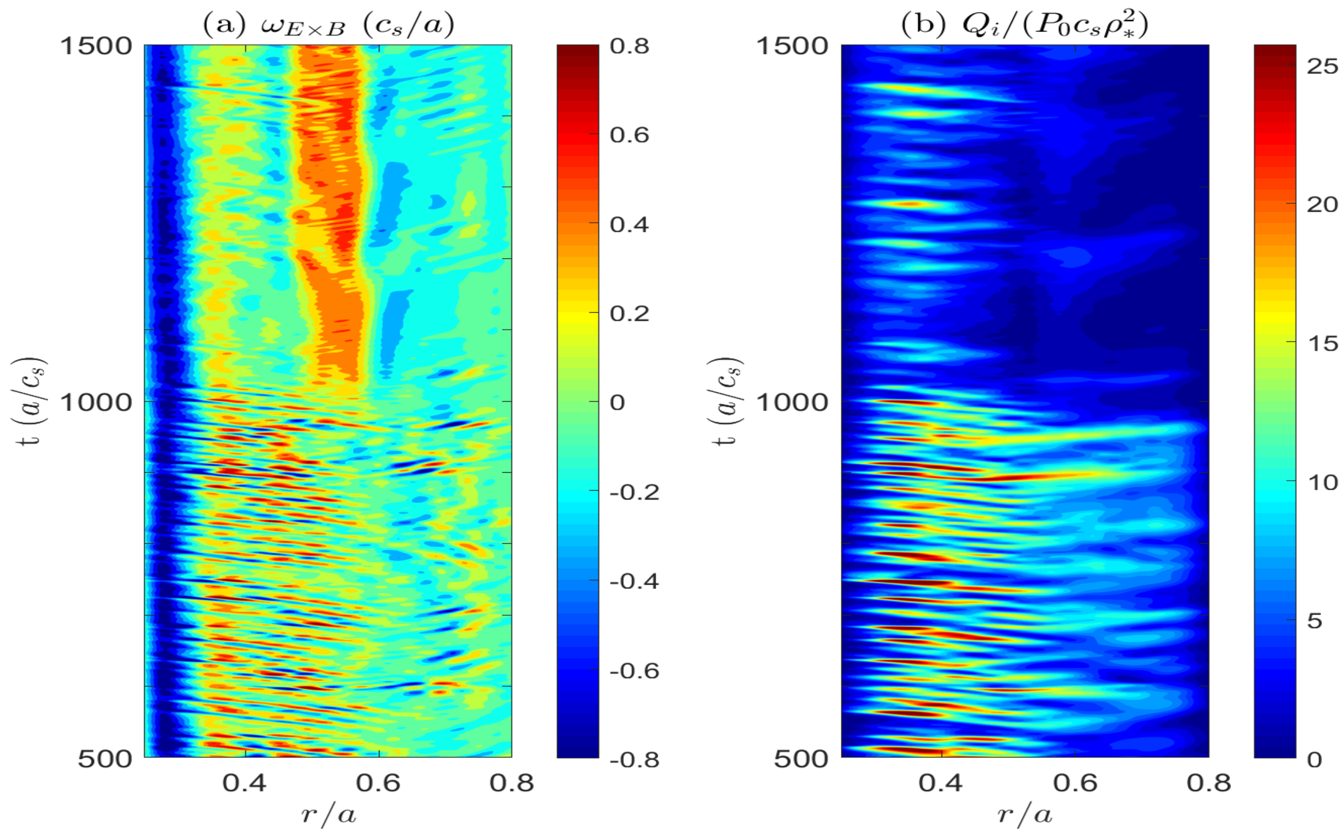

- After strong vorticity injection, stationary zonal flow pattern is formed in a global region due to the vorticity transport by the vorticity injection.
- Avalanche heat transport is quenched after strong vorticity injection.
  ➔ The enhanced and persistent ExB flow shear after vorticity injection regulates heat transport.

Internal transport barrier formation by an external vorticity source (4)

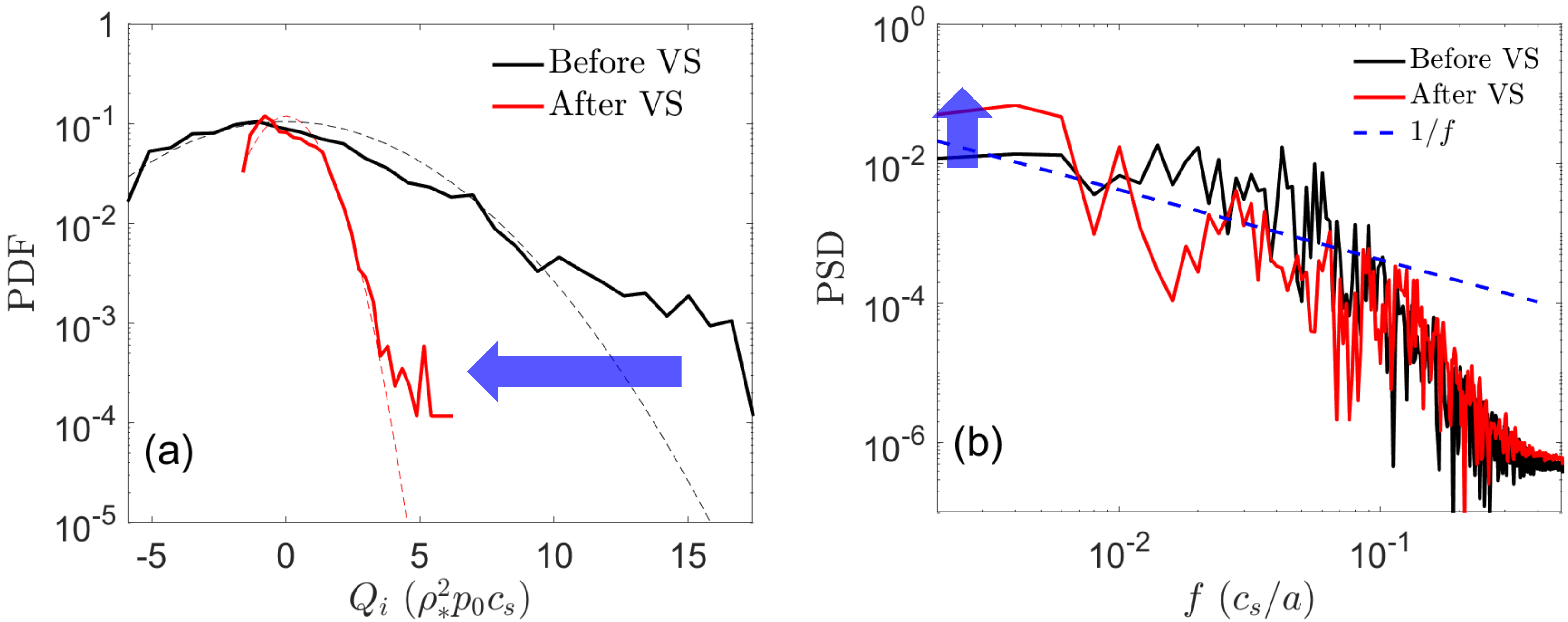

- The strength and the frequency of heat avalanches is reduced in the high confinement regime
  - ➢ VS reduces non-Gaussianity, i.e. (S,K) change from (1.04, 4.72) to (0.56,3.07) and non-Gaussian tail is located at about three times smaller Qi after VS.
  - ➢ Even though both PSD's show broad 1/f region, the PSD at low frequency is about three times higher for the ITB case.
- PDF's and PSD's are calculated using 500 steps in the ITB region before and after vorticity source injection.

Summary

- We developed a 3+1 Global Gyro-Landau Fluid code and showed linear and nonlinear results for global ITG mode.
  - Neoclassical equilibrium is confirmed.
  - Linear and nonlinear ITG thresholds are similar to those of gyrokinetic simulations.
  - Linear ITG threshold $R/L_{T_{i,ctit}} \sim 4$, Nonlinear ITG threshold $R/L_{T_{i,ctit}} \sim 5$ without n=0 potentials.

- In flux-driven simulation, PDF of heat flux is non-Gaussian with (S,K)=(0.768, 4.325) and PSD shows 1/f dependency from low to intermediate frequency range.
  - Self-organized criticality (SOC)-like heat avalanche

- An external vorticity source is considered by solving external vorticity equation separately and coupling with gyrokinetic Poisson equation.
  - ITB is formed by a strong vorticity source injection.
  - The enhanced and persistent ExB flow shear after vorticity injection regulates heat transport.
  - Non-Gaussianity is reduced i.e. (S,K) change from (1.04, 4.72) to (0.56,3.07) and non-Gaussian tail is located at about three times smaller Qi after VS.
  - Even though both PSD's show broad 1/f region, the PSD at low frequency is about three times higher for the ITB case.

Thank you for attention.